Manuscript on

Intrinsic β-catenin overexpression in osteoblast could contribute to impaired osteocytogenesis in Adolescent Idiopathic Scoliosis (AIS)

Authors:

Jiajun Zhang [1,2,3], PhD

Yujia Wang[1,2,3], MSc

Huanxiong Chen [1,2,3], PhD

Bobby Kin-wah Ng [1,2,3], FHKAM

Tsz Ping Lam [1,2,3], FHKAM

Jack Chun-yiu Cheng [1,2,3], MD

Wayne Yuk-wai Lee [1,2,3*], PhD

[1]Department of Orthopaedics and Traumatology, The Chinese University of Hong Kong, Shatin, N.T., Hong Kong

[2]Joint Scoliosis Research Center of the Chinese University of Hong Kong and Nanjing University

[3]SH Ho Scoliosis Research Laboratory, The Chinese University of Hong Kong, Shatin, NT, Hong Kong

Correspondence to the Presenting Author:

Wayne Yuk-wai Lee

Department of Orthopaedics and Traumatology

Rm501, 5/F, Li Ka Shing Medical Sciences Building,

Prince of Wales Hospital,

Shatin, NT,

Hong Kong SAR,

China.

Phone: 852-37636041

Fax: 852-35057889

Email address: waynelee@ort.cuhk.edu.hk

Introduction

Adolescent idiopathic scoliosis (AIS) is a rotational spinal deformity mostly affecting girls during pubertal growth. Though in the majority, the curves will stabilize at skeletal maturity, a certain percentage will progress and require bracing or major surgical treatment. The pathomechanisms underlying the initiation and progression of the spinal deformity remain uncertain. It is of clinical importance to identify the underlying etiopathogenetic mechanisms to inform potential novel prognosticating biomarker, evidence based prevention and treatment strategies.

Since the first report on the relationship between low bone mass and spinal deformity in 1982 (1), cumulative evidence have supported systemic low bone mass as one of the potential mechanisms, affecting multiple skeletal sites in 30-38% of AIS subjects and persist into adulthood thus predisposing to osteoporosis and other related complications in later life (2, 3). Dual-energy X-ray absorptiometry (DXA) measurement indicates that areal bone mineral density (aBMD) at femoral neck is a significant prognostic factor for curve progression (4). Further studies with high-resolution peripheral quantitative computed tomography (HR-pQCT) reveal additional abnormal bone microstructure and bone qualities at distal radius in AIS, including lower cortical area, lower cortical bone volumetric BMD (vBMD), lower trabecular number and larger trabecular separation (5, 6). Recent longitudinal cohort study shows that a cut-off value of cortical vBMD < 570 mgHA/cm^3 at distal radius could increase the prognostic sensitivity and specificity for curve progression to the surgical threshold (7). In view of a good correlation between axial and peripheral bone mass and microstructure (8), it is logical to speculate that vertebra in AIS patients with lower

BMD and deranged bone microstructure might be more vulnerable to asymmetric bone growth and axial vertebral rotation and torsion, and manifested as rotational spinal deformity in the presence of other initiation factors (9). A most recent randomized clinical trial by our group shows that calcium and vitamin D supplementation could prevent curve progression from reaching surgical threshold in AIS with low BMD (*Russell A. Hibbs Clinical Research Award, SRS 2016*) supports further focused mechanistic studies on the bone and bone metabolic pathway.

Recent histomorphometry studies on bone biopsies collected intraoperatively from surgical AIS patients show higher bone turnover and associated larger osteoid area and higher osteoblast number (10, 11), which supported previous observation of abnormal proliferation and osteogenic differentiation ability of primary osteoblast cultures derived from AIS (12, 13). It appears that the osteoblast-lineage cells could play a more important role in the abnormal bone qualities in AIS. Recently, our group reports the aberrant osteocytes and lacuno-canalicular network (LCN) in the iliac crest bone tissues of AIS Vs control subjects (e-poster *#205 SRS 2015*) with state-of-the-art imaging techniques. Osteocytes, the descendant of osteoblasts, are abundant bone cells responsible for mechanosensation and orchestrate bone metabolism through LCN-aided cell to cell communication and paracrine/endocrine signaling. The abnormal osteocytes structure and function together with lower mineralization in bone site where is not primarily affected in AIS suggests a concurrent pathological changes in bone metabolic pathway. The differentiation of osteoblasts into osteocytes (osteocytogenesis) is a tightly regulated process. According to our previous study, one of the most distinctive features in AIS are the

reduced expression of sclerostin in osteocyte. Sclerostin is a potent antagonist to canonical Wnt/β-catenin signaling. Discrepancy in sclerostin expression pattern in AIS osteocyte implies possible dysfunction in Wnt/β-catenin signaling in bone cells (14). With a novel collagen-based three-dimensional (3D) human primary osteocyte culture model (*#66 SRS 2016*), we aimed to investigate the biological role of β-catenin in AIS osteocytogenesis.

Materials and Methods

Subject recruitment

Clinical ethical approval in compliance with the Declaration of Helsinki was obtained from the Ethical Committee of the university and hospital (Ref no. CREC-2014.198). Informed consent was obtained from all subjects. Eleven Chinese AIS girls with severe progressive curves of Cobb angle over 45 degrees undergoing surgical instrumentation and posterior spinal fusion were recruited. Basic anthropometric data, the type of curve, time of occurrence and progression pattern were recorded. Exclusion criteria (15): (a) congenital scoliosis, (b) neuromuscular scoliosis, or (c) scoliosis of metabolic etiology, (d) scoliosis with skeletal dysplasia, or (e) scoliosis with known endocrine and connective tissue abnormalities. Plain radiograph of the whole spine was measured by full length X-ray. Six age- and ethnic-matched non-AIS subjects who required orthopaedic bone related reconstructive surgery were recruited. The CREC specified this in addition to the regular formal consent for the surgical procedure. The control subjects were carefully assessed by two senior orthopaedic clinicians to rule out scoliosis and other known bone metabolic diseases.

Anthropometry, pubertal assessments and curve severity

Anthropometrical parameters including standing height, standing height, body weight and arm span were measured with standardized stadiometric techniques (16). Self-reported pubertal stage was assessed with the guidance of research assistants and pictures according to Tanner Stages (17, 18). For AIS girls, degree of curvature was measured by the Cobb method in the standard standing posteroanterior (PA) radiographs of the whole spine. Cobb angle of the major curve measured within a month before surgery was used for data analysis.

Dual-energy X-ray absorptiometry (DXA)

For all the subjects, aBMD of bilateral femoral necks (g/cm^2) was measured by DXA (XR-46; Norland Medical Systems). The detail of DXA measurement was presented in our previous study (19). Daily calibration was performed and the coefficient of variation was 1.5%. Z-score was calculated with reference to a normative aBMD dataset of local population. The reason not to measure aBMD of the spine is the documented errors associated with axial vertebral rotation that is always present in AIS (20).

Collection of bone biopsy tissues

Trabecular bone biopsies were collected from iliac crests (2 cm anterior to the posterior superior iliac spine) of surgical patients intraoperatively. The iliac bone tissues used in the study were only small piece with actual size less than 1x1x1 cm of the many bone strips taken intraoperatively as part of the standard open surgical iliac bone autograft harvesting for spinal bone fusion for AIS or respective surgical procedure for the controls. In brief, the ilium was exposed surgically and multiple trabecular bone slabs or chips were taken with

chisel and osteotomes from the marrow space with preservation of the iliac crest apophysis and inner wall of the ilium. The surgical procedure was followed by meticulous haemostasis and layered wound closure.

Primary osteoblasts culture

Primary osteoblasts were isolated and cultured as previously stated (21). Bone tissues were cut into small pieces under sterile condition, washed with PBS for three times, and cultured in monolayer in completed alpha-minimum essential medium (α-MEM) consisting of 5% fetal bovine serum (FBS), 1% antibiotics (penicillin, streptomycin and neomycin) and 94 mg/L D-valine (Sigma-Aldrich). At 70% confluence, the cells were split or used for subsequent experiments within five passages. All cell culture reagents were from Thermo Fisher Scientific unless specified.

Determination of osteoblastic activity in monolayer culture

The osteoblastic activity of primary osteoblasts isolated from AIS and control tissues were compared after osteogenic induction (completed α-MEM supplemented with1nM dexamethasone, 50 mM β-glycerophosphate and 1 μM ascorbic acid) (22). Alkaline phosphatase (ALP) activity was determined by ALP colorimetric kit, and extracellular calcium deposits was stained with 2% (w/v) Alizarin red S (pH4.0) and semi-quantified after dissolving in cetylpyridinium chloride solution (23). Results are present by fold change with normalized osteogenic group to non-osteogenic group. Expression level of osteoblastic genes including *Alp*, type I collagen (*Col*), osteopontin (*Spp1*) were determined with qPCR.

All reagents were from Sigma-Aldrich.

Primary osteocytes culture in 3D collagen culture

Primary osteocytes culture was derived from the primary osteoblasts with modified protocol (24). In brief, the osteoblasts were embedded in 2mg/mL type I collagen gel (BD) and cultured in α-MEM supplemented with 5% FBS and 1% antibiotics. Osteocytogenic process was determined by co-immunostaining of ALP (osteoblasts marker) and sclerostin (osteocyte marker), and measurement of released sclerostin in the medium in different time points. At day 7, the osteocytic property was further validated by co-immunostaining of E11 (dendritic marker) and sclerostin. To determine the expression level of osteocytic mRNAs, including *E11*, dentin matrix protein 1 (*Dmp1*), fibroblast growth factor 23 (*Fgf23*) and sclerostin (*Sost*), and intracellular sclerostin expression, the cells were first dissociated from the gel with 2 mg/mL type I collagenase (Sigma-Aldrich) at 37°C for 10 min and pelleted at 170 g for 10 min.

RNA oligoribonucleotides and cell transfection

Loss of function model was achieved with small interfering RNA (siRNA) (Genepharma). Three different pairs of siRNA sequences were designed to test the efficiency for the knock down of target human β-catenin mRNA (*Ctnnb1*). The most effective pair was selected. A negative control duplex (NC) was applied to each study. Sequence for RNA oligoribonucleotides is listed in table 3. Primary osteoblasts was seeded in 24 well plate. At 50% confluence, 1 ug siRNA or NC was delivered by lipofectamine 3000 (Life

Technologies). The transfected osteoblasts was detached after 24 h and embedded in collagen gel for the assessment of osteocytic activities.

RNA extraction and real time qPCR

Freshly snap frozen bone tissues were ground with autoclaved pestle and mortar in the presence of liquid nitrogen. Total RNA from bone tissues and primary cell cultures were extracted with Trizol (Life Technologies) according to manufacturer's protocol. Reverse transcriptase (Takara-bio) was used for the conversion to cDNA. Transcriptional level of representative osteogenic and osteocytic markers were determined by real time qPCR with Power SYBR® Green (Life Technologies). Expression levels of *Sost* were detected with Taqman probe (Life Technologies). In brief, after denaturation at 94°C for 10 min, the qPCR was conducted in 45 cycles of 95°C for 15s (denaturation) and 60°C for 60 s (annealing and elongation). The relative expression level was normalized to glyceraldehyde 3-phosphate dehydrogenase (Gapdh). The primer sequence and related information are listed in table 4.

Western blot

Total soluble protein was extracted with ice cold lysis buffer (1% NP-40, 10 mM HEPES, 60 mM KCl and protease inhibitor, Sigma-Aldrich). Cell debris was removed by centrifugation at 15000 g for 15 min at 4°C. To extract cytosolic fraction, 60 ul cytoplasmic extraction buffer (10mM HEPES, 6 0mM KCl, 1 mM EDTA and 0.25% NP40) was added for cell lysis. After 5 min lysis on ice, the cytosolic fraction was collected by centrifugation at 2600 rpm for 4 min at 4°C. 20 ug protein was subjected to SDS-PAGE and transferred to

PVDF membrane. The membrane was blocked with 5% (w/v) non-fat dry milk in Tris-buffered saline with Tween 20 (TBST) for 1 h before incubation with primary antibodies against sclerostin (Ab63097, Abcam) or connexin43 (MAB3067, EMD Millipore), for overnight at 4°C. The membrane was probed with secondary antibody at room temperature for 1hr. ECL substrate (GE Healthcare) was used to detect protein bands. Semi-quantification analysis was performed using Image J (NIH)

Statistical analysis

All results were presented in mean ± standard deviation. Mann-Whitney *U* test was used because of relatively small sample size. The statistical analyses was conducted using SPSS 19.0 (IBM, NY). Significance level was set at $p<0.05$.

Results

In this study, six non-AIS subjects undergoing different orthopaedic surgery requiring iliac crest autografts were included (four male subjects and two female subjects) (Table 1). AIS and control subjects had similar anthropometric, pubertal and radiological parameters, but AIS had lower aBMD value at non-dominant femoral neck (Table 2).

Standard osteogenic induction experiment supported the observation of abnormal osteoblastic ability of AIS osteoblasts (Figure 1). In ALP activity test, AIS osteoblasts showed consistently lower ALP activity in a temporal sequence though not reaching statistical significance. Calcium deposition capacity indicated by Alizarin Red staining

(ARS) showed significantly lower *(p=0.021)* level of extracellular calcium deposits at day 14 under osteogenic induction in AIS osteoblast when compared with that in controls. In addition, AIS osteoblasts exhibited significantly higher mRNA level of *Col1* (*p=0.018*) after 4 day culture and reduced mRNA expression of *Spp1* (*p=0.02*) after 7 days culture with osteogenic medium.

Based on our previous reported modified protocol (*#66 SRS 2016),* we conducted a time-course study to determine the optimal incubation period to obtain mature osteocytes for subsequent studies. Figure 2 illustrates the process to induce osteocytogenic differentiation in 3D collagen gel. Figure 3a shows the changes of ALP positive and sclerostin positive cells in 3D collagen gel during at day 3, 7 and 14 after seeding primary osteoblasts in the gel. Co-immunostaining showed time dependent increase in *Sost* mRNA and decrease in *Alp* mRNA. This change was further supported by significant increased sclerostin release in the 3D collagen culture which was undetectable in the monolayer culture (Figure 3b). In the 3D culture, the level of released sclerostin reached the peak at day 7 (19.88±15.62 pg/ml) and remained steady until day 14 (17.56±2.93 pg/ml).

To validate whether the current model could resemble near native microenvironment and replicate pathological changes in bone disease *in vitro,* primary osteocytes from AIS subjects were cultured and compared to that from non-AIS subjects in terms of osteocyte activities. Representative functional osteocytic markers, *Dmp1, Sost* and *Fgf23* are closely associated with mineralization and bone qualities. Aberrant osteocyte activities in AIS was suggested by reduced mRNA level of functional markers, *Dmp1*, *Sost* and *Fgf23* in AIS trabecular bone biopsies when compared with that in controls (Figure 4). Similar declined

trend of interested functional markers, *Sos*t and *Fgf23*, was resembled in 3D primary osteocyte culture of AIS, which indicated that the 3D primary osteocyte culture possessed the ability to reveal pathological abnormalities in AIS osteocytes *in vitro*. Furthermore, AIS osteocytes exhibited lower level of E11 and connexin43 (and its mRNA *Gja1*), suggesting defective dendrite formation and connectivity (Figure 5)

In the present study, we did observe persistent higher mRNA level of *Ctnnb1* and active β-catenin protein in bone tissues and primary osteoblasts in AIS. Figure 6 showed that AIS expressed significantly higher transcriptional level of β-catenin (*Ctnnb1*) at bone tissue (*p=0.002*) and primary osteoblast culture (p=0.045) which are consistent to immunostaining of active β-catenin in the bone tissues. Western blot result confirmed higher protein level of active form of β-catenin in the cytosolic fraction in AIS primary osteoblast culture (*p=0.021*).

Three days after transfection, loss of function model was successfully established in human primary osteoblast culture as indicated by reduction in *Ctnnb1* level (*p=0.009*) when compared with corresponding control group. Knock down of *Ctnnb1* partially rescued the decline levels of *E11* (*p=0.021*) and *Spp1* (*p=0.042*) in AIS osteoblasts. Similar effects were also observed in the control osteoblasts but not reaching significant power. AIS primary osteoblasts with *Ctnnb1* knockdown showed profound increase in *Sost* expression (*p=0.021*) and sclerostin release (*p=0.006*) under osteocytogenic condition, suggesting the impact of overexpression of β-catenin on osteocytogenic differentiation in AIS (figure 7).

Discussion

In previous study, we found structural and morphological defect in osteocytes LCN and reduced sclerostin expression in AIS (unpublished data). To characterize the pathological function of osteocyte in AIS, we refined a human primary 3D osteocyte model from bone tissues, which could resemble osteocytic features and retain some pathological alterations of osteocyte in AIS. In this study, we also revealed the persistent overexpression of β-catenin in AIS osteoblasts which might partly contribute to the abnormal osteoblastic activity and osteocytogenic differentiation as indicated by loss of function study.

In contrast to previous primary osteoblasts study collected from different anatomical sites (25), our results from site-matched bone samples revealed aberrant overexpression of β-catenin and impaired osteocytogenic differentiation in AIS. The link between scoliosis and β-catenin activity via *ptk7* disruption has been reported in zebrafish model (26). Another group reports an AIS susceptible locus near *tnik* (27), which is co-activator of β-catenin/Tcf4 transcriptional complex (28). Sclerostin as a potent inhibitor of canonical Wnt/β-catenin signaling (29), the decreased sclerostin in AIS osteocytes might lead to over-activation of the β-catenin signaling pathway and exhibit a paradoxical inhibitory effect on osteoblasts differentiation(30) (31) and bone tissue mineralization (32). β-catenin activation in osteoblasts is generally believed to increases bone mass, whereas inactivation decreases bone mass (30), but cumulative evidence suggests that over-activation of β-catenin signaling could also result in lower bone mass (32). Regards *et al* has similar observation in human fibrous dysplasia (FD). Overexpression of β-catenin in osteoblast precursors has been demonstrated in FD, a skeletal disease resulted from mutation in *GNAS*. Skeletal phenotype

of FD is associated with abnormal bone qualities, low bone mineral density and high bone turn over. Such abnormal differentiation could be rescued after decreasing the β-catenin signaling in osteoblast progenitors.

In conclusion, this study demonstrated overexpression β-catenin in AIS osteoblast and decreased sclerostin production and secretion in AIS osteocyte. With loss of function assay of β-catenin in AIS osteoblast, we proved that overexpression β-catenin was associated with reduced sclerostin secretion in AIS. Given that Wnt/β-catenin signaling pathway is a well-known molecular oscillator regulating periodic vertebrate segmentation (reviewed in (33)) and plays important roles particularly in skeletal development and disease (34), it is reasonable to hypothesize that the abnormal osteocytogenesis and β-catenin dysfunction observed in this study could play an important role in the etiopathogenesis of AIS at the peri-pubertal period in the presence of other triggering factors. Further study is warranted to investigate the possible upstream environmental factors and other intrinsic factors that could account for the clinical and biological observations in AIS.

Figure legend

Table 1. Basic information of non-AIS control subjects

Case No.	Diagnosis	Gender	Age (years)
Control 1	Lumbar vertebral fracture	Male	19
Control 2	Lumbar spondylolisthesis	Male	10
Control 3	Lumbar spondylolisthesis	Male	12
Control 4	Lumbar spondylolisthesis	Female	12
Control 5	Left scapula osteomyelitis	Male	13
Control 6	L1 compression fracture	Female	24

Table 2. Anthropometric, pubertal and radiological assessment in controls and AIS.

	Control (N=6, 2F & 4M)		AIS (N=11, Female)		
	Mean	SD	Mean	SD	*p* value
Age	15.00	5.37	15.20	1.69	0.313
Standing height (cm)	163.10	5.92	156.59	5.71	0.055
Body weight (kg)	51.58	23.11	49.99	12.90	0.852
Arm span (cm)	161.08	5.23	157.61	5.62	0.412
LtFNBMD (z-score)	-1.85	0.51	-0.40	0.99	0.020
Cobb angle (º)	-	-	48.00	5.89	
Tanner Stage	3.17	1.47	3.90	0.99	0.220
Breast Stage	3.67	1.21	3.80	0.79	0.875

Abbreviation: LtFNBMD: left femoral neck aBMD;
Data was expressed as mean ± SD;
Mann–Whitney test was used in comparison.

Table 3. Sequence for RNA oligoribonucleotides.

Target Gene	Sequence
Ctnnb1	5'-UAAUGAGGACCUAUACUUATT-3'
	5'-UAAGUAUAGGUCCUCAUUATT-3'

Abbreviation: Ctnnb1 is mRNA for β-catenin

Table 4. Primer sequences.

Gene		Sequence (From5'-3')	NCBI (NM)
Alp	Forward	ACCTGCTTTATCCCTGGAGC	000478.5
	Reverse	CTTGTGCCTGGACGGAC	
Col1	Forward	GTCACCCACCGACCAAGAAACC	000088.3
	Reverse	AAGTCCAGGCTGTCCAGGGATG	
E11	Forward	CTATAAGTCTGGCTTGACAACTCTG	006474.4
	Reverse	TCACTGTTGACAAACCATCTTTCTC	
Gja1	Forward	CCCTCCAGCAGTTGAGTAGG	000165.4
	Reverse	GGAGTTCAATCACTTGGCGT	
Dmp1	Forward	AGCATCCTGCTCATGTTCCTTT	004407.3
	Reverse	GAGCCAAATGACCCTTCCATT	
Spp1	Forward	CTAGGCATCACCTGTGCCATACC	001251829.1
	Reverse	CAGTGACCAGTTCATCAGATTCATC	
Fgf23	Forward	TAATCACCACAAAGCCAGCA	020638.2
	Reverse	CACCTGCAGATCCACAAGAA	
Sost		TAQMAN	Hs00228830_m1
Gapdh	Forward	TGCACCACCAACTGCTTAGC	
	Reverse	GGCATGGACTGTGGTCATGAG	

Abbreviation: *Alp*, alkaline phosphatase mRNA; *Col1*, type I collagen mRNA, *E11*, E11 glycoprotein mRNA; *Gja1*, connexin43 mRNA; *Dmp1*, dentin matrix protein 1 mRNA; *Spp1*, osteopontin mRNA; *Fgf23*, fibroblast growth factor 23 mRNA; *Sost*, sclerostin mRNA; *Gapdh*, glyceraldehyde 3-phosphate dehydrogenase mRNA.

Figure 1

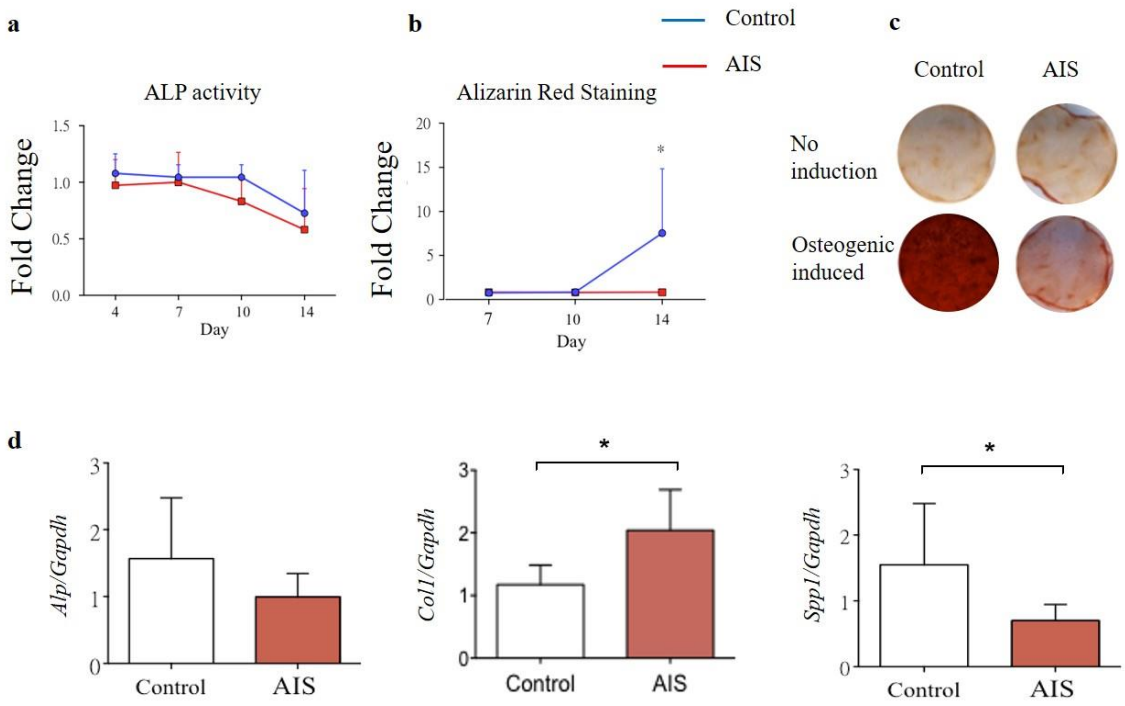

Figure 1. Comparing osteoblastic ability of primary osteoblast from AIS and controls. (a) Semi-quantitative analysis of ALP activity of primary osteoblasts from AIS and control under osteogenic induction in temporal sequence shows similar ALP activity between AIS and control. (b) Semi-quantitative analysis of calcium deposits stained with ARS shows significantly decreased mineralization ability of AIS osteoblasts. Fold change is calculated by dividing osteogenic relative by non-osteogenic group. (c) Representative images of ARS staining. (d) Representative osteoblastic markers expression. AIS osteoblasts express higher mRNA level of (a) *Col1*, reduced level of *Alp*, significantly declined level of *Spp1*. Data are expressed as mean ± SD. * $p<0.05$. N = 11 AIS and 6 controls.

Figure 2

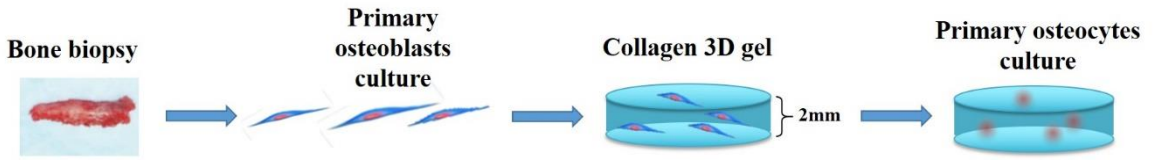

Figure 2. Schematic illustration of osteocytogenesis *in vitro*. Freshly harvested bone biopsy from control or AIS subjects were subjected to primary osteoblasts culture by explant culture technique. The osteoblasts characterized by alkaline phosphatase (ALP) staining were collected and seeded in collagen-based 3D culture in order to facilitate osteocytogenic differentiation toward osteocytes.

Figure 3

3a

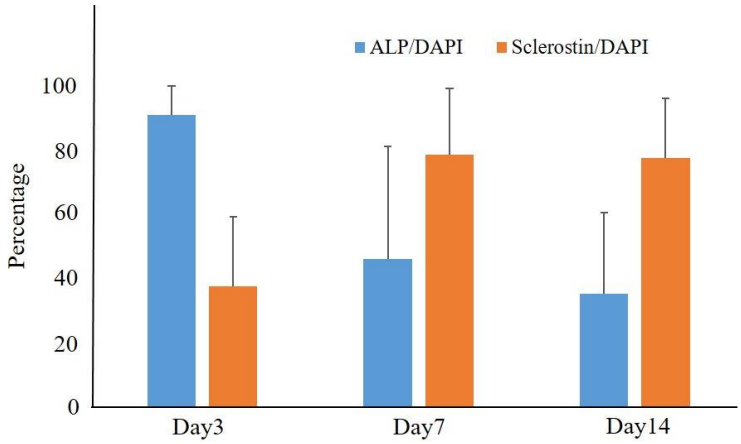

3b

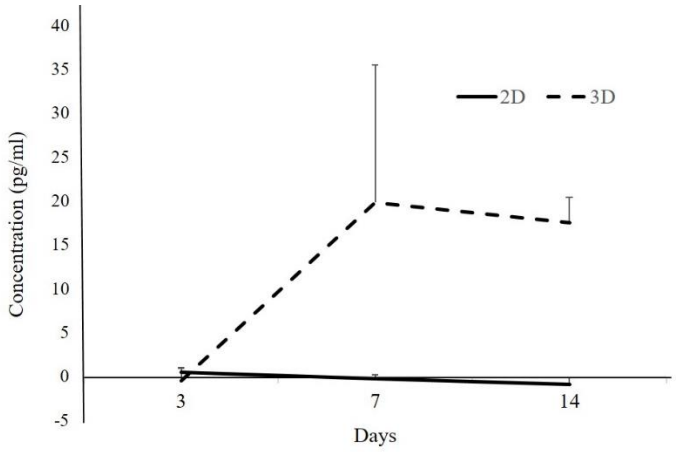

Figure 3. Temporal changes in human primary osteocytes culture. (a) Percentage of ALP positive and sclerostin positive cells after 3, 7 or 14 days of 3D culture in collagen gel. Five field of view per sample were randomly selected and counted by blinded examiner. A increasing trend of sclerostin positive cells and a decreasing trend of ALP positive cells were found after 2 weeks of culture. (b) Level of released sclerostin in culture medium. Primary osteocytes culture in 3D culture significantly secreted more sclerostin when compared to

osteoblasts cultured in 2D monolayer culture. Sclerostin is undetectable in conditioned medium of monolayer osteoblast culture. Data are expressed as mean ± SD. N = 3 controls

Figure 4

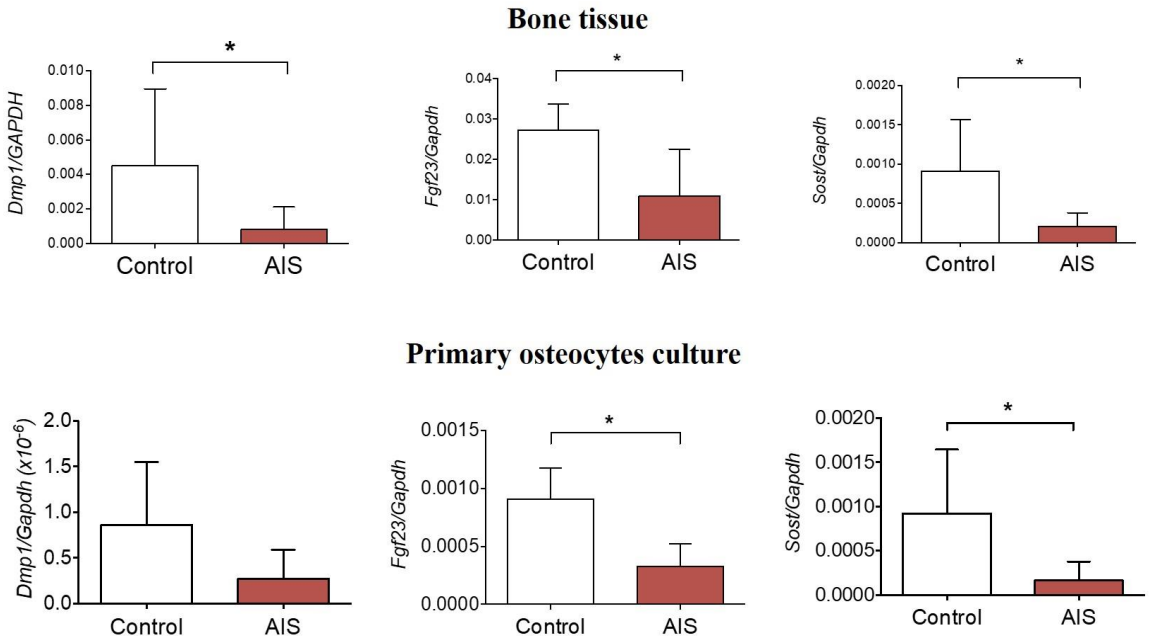

Figure 4. Comparing osteocytic markers expression level between primary osteocytes culture and bone tissues which the cells derived from. (a) mRNA levels of *Dmp1*, *Fgf23* and *Sost* in bone tissues from AIS and control; (b) mRNA levels of *Dmp1*, *Fgf23* and *Sost* in primary osteocytes culture from AIS and control. AIS has lower expression level of *Dmp1*, *Fgf23* and *Sost* in both tissue and cellular levels when compared to that in control. Data are expressed as mean ± SD. **p*<0.05. N = 11 AIS and 6 controls.

Figure 5

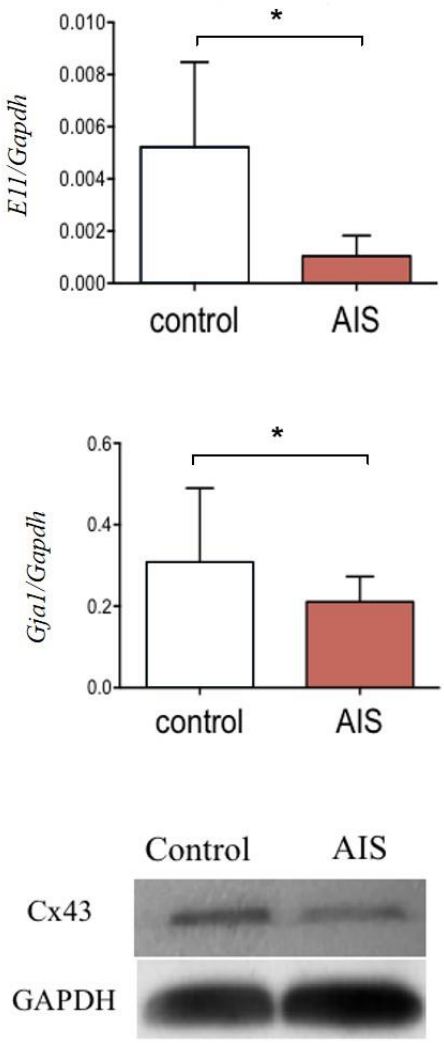

Figure 5. Reduced mRNA expression level of *E11*, and mRNA and protein level of Cx43 (*Gja1*) in AIS osteocytes. *E11* and *Gja1* are representative mRNA markers for dendritic formation and cell to cell communication. Data are expressed as mean ± SD. *$p<0.05$. N = 11 AIS and 6 controls.

Figure 6

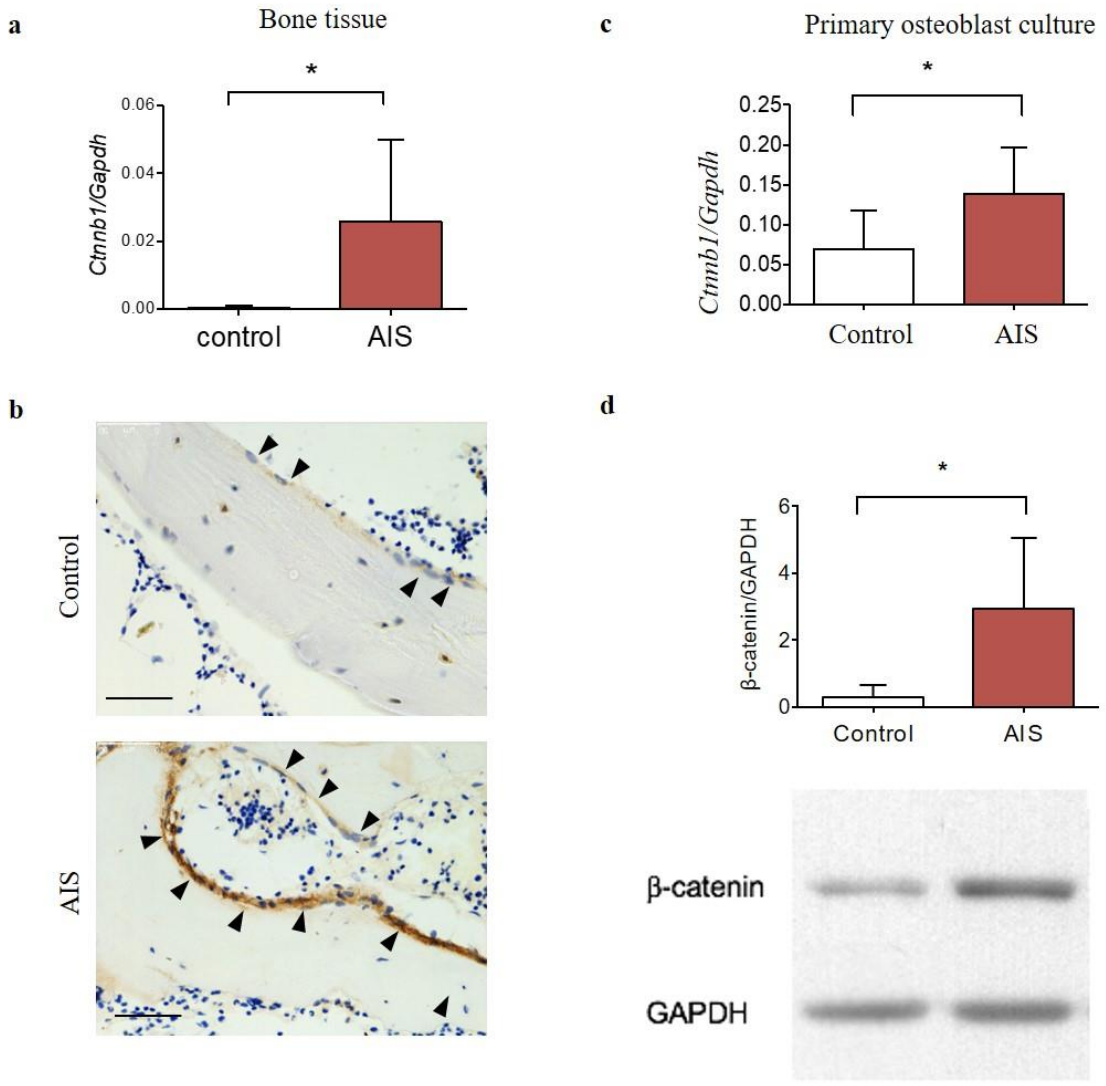

Figure 6. Elevated β-catenin expression in AIS. (a) Higher *Ctnnb1* mRNA level in AIS bone tissues and more active β-catenin in bone lining cells in AIS bone tissues. Representative immunostaining images shows the increased expression of active β-catenin (arrows) in the lining cells, but less differential in the osteocytes in AIS bone biopsies. Scale bar, 50μm. Higher expression level of (c) *Ctnnb1* and (d) cytosolic active β-catenin in AIS primary osteoblasts culture. Representative Western blot image for semi-quantiatation of cytosolic active β-catenin expression level. Data are expressed as mean ± SD. *p<0.05. N = 11 AIS and 6 controls.

Figure 7

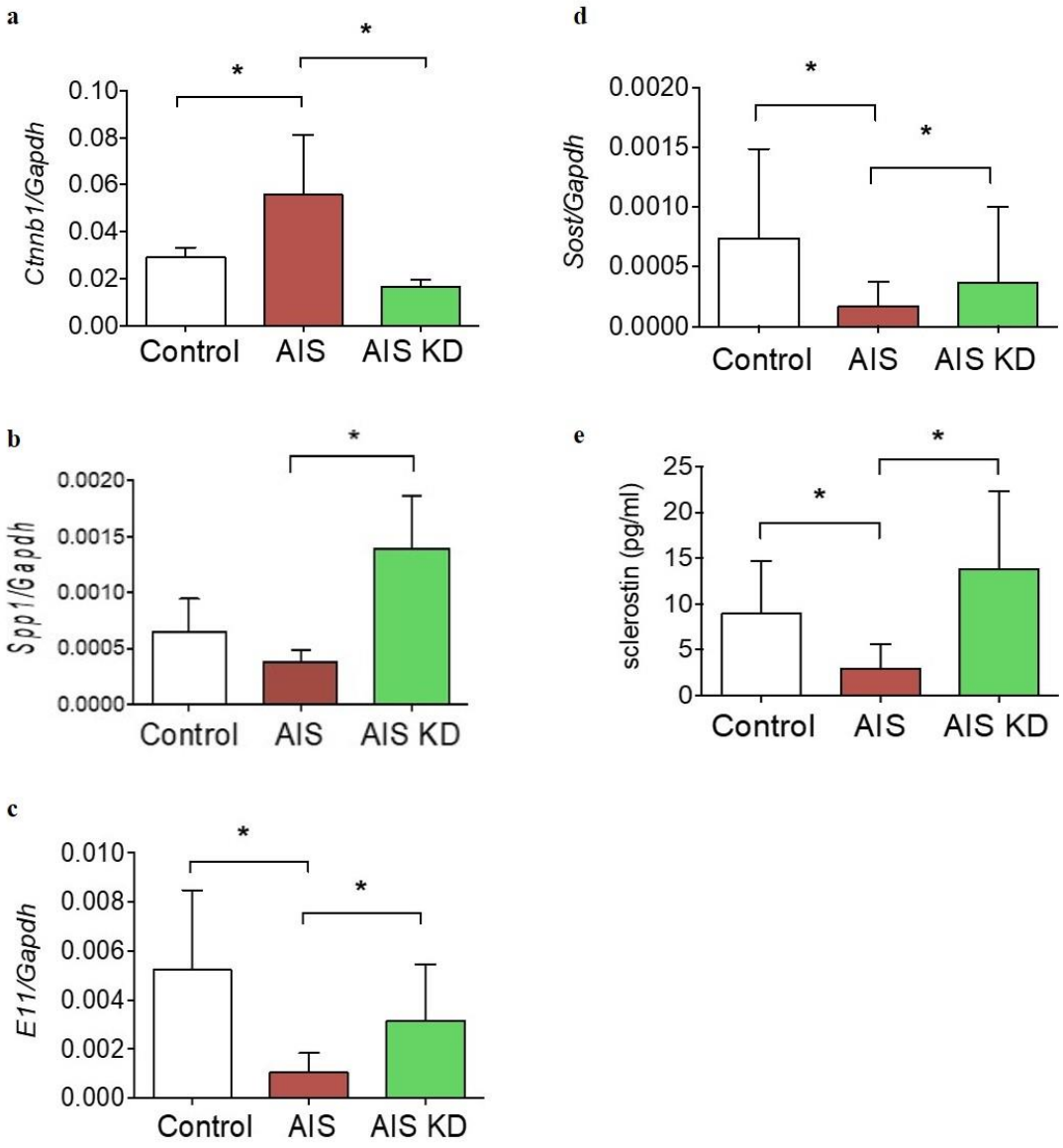

Figure 7. Knockdown of β-catenin in AIS osteoblast partially rescued osteoblastic genes expression and osteocytic activity. (a) Decreased C*tnnb1* expression in control and AIS osteoblasts after transfection of siRNA targeting *Ctnnb1*. (b) Increased mRNA expression of osteoblast E11 and Spp1 after the knock down of *Ctnnb1* in AIS osteoblasts. (c) Knockdown of *Ctnnb1* in AIS osteoblasts partly rescued the impaired sclerostin release in AIS osteocytes. . Data are expressed as mean ± SD. **p*<0.05. N = 11 AIS and 6 controls.

References

1. Burner WL, 3rd, Badger VM, Sherman FC. Osteoporosis and acquired back deformities. J Pediatr Orthop. 1982;2(4):383-5.
2. Cheng JC, Guo X, Sher AH. Persistent osteopenia in adolescent idiopathic scoliosis. A longitudinal follow up study. Spine (Phila Pa 1976). 1999;24(12):1218-22.
3. Thomas KA, Cook SD, Skalley TC, Renshaw SV, Makuch RS, Gross M, et al. Lumbar spine and femoral neck bone mineral density in idiopathic scoliosis: a follow-up study. Journal of pediatric orthopedics. 1992;12(2):235-40.
4. Hung VW, Qin L, Cheung CS, Lam TP, Ng BK, Tse YK, et al. Osteopenia: a new prognostic factor of curve progression in adolescent idiopathic scoliosis. The Journal of bone and joint surgery American volume. 2005;87(12):2709-16.
5. Yu WS, Chan KY, Yu FWP, Ng BKW, Lee KM, Qin L, et al. Bone structural and mechanical indices in Adolescent Idiopathic Scoliosis evaluated by high-resolution peripheral quantitative computed tomography (HR-pQCT). Bone. 2014;61:109-15.
6. Wang ZW, Lee WY, Lam TP, Yip BH, Yu FW, Yu WS, et al. Defining the bone morphometry, micro-architecture and volumetric density profile in osteopenic vs non-osteopenic adolescent idiopathic scoliosis. Eur Spine J. 2016.
7. Yip BH, Yu FW, Wang Z, Hung VW, Lam TP, Ng BK, et al. Prognostic Value of Bone Mineral Density on Curve Progression: A Longitudinal Cohort Study of 513 Girls with Adolescent Idiopathic Scoliosis. Sci Rep. 2016;6:39220.
8. Liu XS, Cohen A, Shane E, Yin PT, Stein EM, Rogers H, et al. Bone Density, Geometry, Microstructure, and Stiffness: Relationships Between Peripheral and Central Skeletal Sites Assessed by DXA, HR-pQCT, and cQCT in Premenopausal Women. Journal of Bone and Mineral Research. 2010;25(10):2229-38.
9. Cheng JC, Castelein RM, Chu WC, Danielsson AJ, Dobbs MB, Grivas TB, et al. Adolescent idiopathic scoliosis. Nature Reviews Disease Primers. 2015:15068.
10.Tanabe H, Aota Y, Nakamura N, Saito T. A histomorphometric study of the cancellous spinal process bone in adolescent idiopathic scoliosis. Eur Spine J. 2017.
11.Wang Z, Chen H, Yu YE, Zhang J, Cheuk K-Y, Ng BK, et al. Unique local bone tissue characteristics in iliac crest bone biopsy from adolescent idiopathic scoliosis with severe spinal deformity. Scientific Reports. 2017;7.
12.Letellier K, Azeddine B, Parent S, Labelle H, Rompre PH, Moreau A, et al. Estrogen cross-talk with the melatonin signaling pathway in human osteoblasts derived from adolescent idiopathic scoliosis patients. J Pineal Res. 2008;45(4):383-93.
13.Man GC, Wang WW, Yeung BH, Lee SK, Ng BK, Hung WY, et al. Abnormal proliferation and differentiation of osteoblasts from girls with adolescent idiopathic scoliosis to melatonin. J Pineal Res. 2010;49(1):69-77.
14.Compton JT, Lee FY. A review of osteocyte function and the emerging importance of sclerostin. The Journal of bone and joint surgery American volume. 2014;96(19):1659-68.
15.Iwasaki S, Nakazawa K, Sakai J, Kometani K, Iwashita M, Yoshimura Y, et al. Melatonin as a local regulator of human placental function. Journal of Pineal Research. 2005;39(3):261-5.
16.Siu King Cheung C, Tak Keung Lee W, Kit Tse Y, Ping Tang S, Man Lee K, Guo X, et al. Abnormal peri-pubertal anthropometric measurements and growth pattern in adolescent idiopathic scoliosis: a study of 598 patients. Spine (Phila Pa 1976). 2003;28(18):2152-7.
17.Tanner JM. Normal growth and techniques of growth assessment. Clin Endocrinol Metab. 1986;15(3):411-51.
18.Marshall WA, Tanner JM. Variations in pattern of pubertal changes in girls. Arch Dis Child. 1969;44(235):291-303.
19.Yu WS, Chan KY, Yu FW, Ng BK, Lee KM, Qin L, et al. Bone structural and mechanical indices in Adolescent Idiopathic Scoliosis evaluated by high-resolution peripheral quantitative computed tomography (HR-pQCT). Bone. 2014;61:109-15.

20.Cheng JC, Sher HL, Guo X, Hung VW, Cheung AY. The effect of vertebral rotation of the lumbar spine on dual energy X-ray absorptiometry measurements: observational study. Hong Kong Med J. 2001;7(3):241-5.
21.Man GC, Wong JH, Wang WW, Sun GQ, Yeung BH, Ng TB, et al. Abnormal melatonin receptor 1B expression in osteoblasts from girls with adolescent idiopathic scoliosis. Journal of pineal research. 2011;50(4):395-402.
22.Lau E, Lee WD, Li J, Xiao A, Davies JE, Wu Q, et al. Effect of low-magnitude, high-frequency vibration on osteogenic differentiation of rat mesenchymal stromal cells. J Orthop Res. 2011;29(7):1075-80.
23.Stanford CM, Jacobson PA, Eanes ED, Lembke LA, Midura RJ. Rapidly forming apatitic mineral in an osteoblastic cell line (UMR 106-01 BSP). The Journal of biological chemistry. 1995;270(16):9420-8.
24.Uchihashi K, Aoki S, Matsunobu A, Toda S. Osteoblast migration into type I collagen gel and differentiation to osteocyte-like cells within a self-produced mineralized matrix: a novel system for analyzing differentiation from osteoblast to osteocyte. Bone. 2013;52(1):102-10.
25.Oliazadeh N, Gorman KF, Eveleigh R, Bourque G, Moreau A. Identification of Elongated Primary Cilia with Impaired Mechanotransduction in Idiopathic Scoliosis Patients. Sci Rep. 2017;7:44260.
26.Hayes M, Gao X, Yu LX, Paria N, Henkelman RM, Wise CA, et al. ptk7 mutant zebrafish models of congenital and idiopathic scoliosis implicate dysregulated Wnt signalling in disease. Nature communications. 2014;5:4777.
27.Zhu Z, Xu L, Leung-Sang Tang N, Qin X, Feng Z, Sun W, et al. Genome-wide association study identifies novel susceptible loci and highlights Wnt/beta-catenin pathway in the development of adolescent idiopathic scoliosis. Hum Mol Genet. 2017;26(8):1577-83.
28.Mahmoudi T, Li VS, Ng SS, Taouatas N, Vries RG, Mohammed S, et al. The kinase TNIK is an essential activator of Wnt target genes. EMBO J. 2009;28(21):3329-40.
29.Poole KE, van Bezooijen RL, Loveridge N, Hamersma H, Papapoulos SE, Lowik CW, et al. Sclerostin is a delayed secreted product of osteocytes that inhibits bone formation. FASEB journal : official publication of the Federation of American Societies for Experimental Biology. 2005;19(13):1842-4.
30.Baron R, Kneissel M. WNT signaling in bone homeostasis and disease: from human mutations to treatments. Nat Med. 2013;19(2):179-92.
31.Boland GM, Perkins G, Hall DJ, Tuan RS. Wnt 3a promotes proliferation and suppresses osteogenic differentiation of adult human mesenchymal stem cells. J Cell Biochem. 2004;93(6):1210-30.
32.Regard JB, Cherman N, Palmer D, Kuznetsov SA, Celi FS, Guettier JM, et al. Wnt/beta-catenin signaling is differentially regulated by Galpha proteins and contributes to fibrous dysplasia. Proc Natl Acad Sci U S A. 2011;108(50):20101-6.
33.Pourquie O. Vertebrate segmentation: from cyclic gene networks to scoliosis. Cell. 2011;145(5):650-63.
34.Yang Y. Wnt signaling in development and disease. Cell Biosci. 2012;2(1):14.